Journal of Solid State Chemistry **142,** 120–129 (1999)
Article ID jssc.1998.7995, available online at http://www.idealibrary.com on IDEAL®

Elaboration, Structures, and Phase Transitions for YFe_2D_x Compounds ($x = 1.3$, 1.75, 1.9, 2.6) Studied by Neutron Diffraction

V. Paul-Boncour,*,[1] L. Guénée,*,[2] M. Latroche,* A. Percheron-Guégan,* B. Ouladdiaf,† and F. Bourée-Vigneron‡

*Laboratoire de Chimie Métallurgique des Terres Rares, CNRS, 2-8 rue H. Dunant, F-94320 Thiais Cedex, France and †Institut Laue Langevin, Av. des Martyrs, BP 156, F-38042 Grenoble Cedex 9, France; and ‡Laboratoire Léon-Brillouin, CNRS, CE-Saclay, F-91191 Gif sur Yvette Cedex, France

Received April 24, 1998; in revised form July 24, 1998; accepted August 3, 1998

The structure of YFe_2D_x deuterides ($x = 1.3$, 1.9, 1.75, and 2.6) have been studied by neutron diffraction (ND). The influence of a thermal treatment on the synthesis of YFe_2D_x deuterides has been followed by *in situ* neutron diffraction for $x = 1.3$ and 1.9. After deuterium absorption at room temperature, their diffraction patterns show a mixture of YFe_2 and a deuteride phase YFe_2D_y ($2.3 < y < 2.6$). Heating the samples above 400 K for $x = 1.3$ and 425 K for $x = 1.9$, leads to a deuterium diffusion from the deuterium rich phase toward YFe_2 to form a single phase deuteride with lower D content. Single phase deuterides $YFe_2D_{1.3}$, $YFe_2D_{1.75}$, and $YFe_2D_{1.9}$ display superstructure lines which imply a lowering of symmetry compared to the cubic C15 structure of the parent intermetallic. $YFe_2D_{1.3}$ crystallizes in the tetragonal $I\bar{4}$ space group ($Z = 20$) with $a = 11.985(2)$ Å and $c = 7.622(1)$ Å, $YFe_2D_{1.75}$ in the cubic $I\bar{4}3m$ space group ($Z = 64$) with $a = 15.336(2)$ Å, and $YFe_2D_{1.9}$ in a tetragonal structure with $a = 12.145(2)$ Å and $c = 23.064(2)$ Å. The analysis of their ND patterns at 300 K shows for $x = 1.3$ and 1.75 an ordering of the deuterium atoms in some preferential tetrahedral Y2Fe2 sites and a ferromagnetic structure with 1.5 and 1.9 μB/Fe, respectively. For $YFe_2D_{1.3}$ and $YFe_2D_{1.9}$ the superstructure lines disappear above 460 and 444 K, respectively, and they return to a C15 structure. The origin of the structural deviation and of the order–disorder transition is discussed in relation with deuterium and magnetic ordering. $YFe_2D_{2.6}$ deuteride crystallizes at 300 K in the cubic $Fd3m$ space group ($Z = 8$) with $a = 7.785(2)$, deuterium atoms located statistically in tetrahedral Y2Fe2 sites and a ferromagnetic structure with a magnetic moment of 1.8 μB/Fe.

Key Words: **hydride; Laves phase; neutron diffraction.**

1. INTRODUCTION

The influence of hydrogen absorption on the structural and magnetic properties of RFe_2 compounds (R = rare earth) has been the subject of several works (1–3). In this field the study of the YFe_2–H_2 system is of particular interest since it makes it possible to study the influence of hydrogen absorption on the magnetic Fe sublattice. Increasing the hydrogen content makes it possible to increase the Fe–Fe interatomic distances which can be considered as applying a "negative pressure." In order to build the YFe_2–H_2 phase diagram several studies have already been performed and will be summarized.

First, Fe_2D_x hydrides with various hydrogen (deuterium) contents were prepared by absorption at room temperature. A mixture of YFe_2 and YFe_2D_y was always obtained for $x < 3.3$, whereas for $x > 3.3$ single phase rhombohedral hydrides can be prepared. Therefore in order to obtain single phase deuterides with $x < 3.3$ a thermal treatment has been applied after hydrogenation at room temperature (4, 5). The influence of the annealing temperature was studied in details in Ref. 4 for $YFe_2D_{1.3}$. A correlation was established between the structural evolution as a function of temperature and the pressure variation during the heating treatment. A thermal treatment at 408 K or deuterium absorption at 408 K allow to obtain single phase deuterides for some definite concentrations. The X-ray diffraction (XRD) patterns of some of these deuterides display weak tetragonal distortions and superstructure lines, leading to new structures derived from the cubic C15 structure of YFe_2. $YFe_2D_{1.3}$ was found to crystallize in a tetragonal cell ($a = 11.98$ and $c = 7.61$ Å), $YFe_2D_{1.75}$ and $YFe_2D_{1.9}$ in a cubic structure with a double cell parameter ($a = 15.34$ and 15.38 Å, respectively). For $2.5 \leq x \leq 2.9$ the XRD patterns were refined in the cubic C15 structure. The existence of several two phase ranges for intermediate deuterium content was related to the multiplateau behavior of the YFe_2D_x pressure–composition isotherms (4, 5). In addition local order studies by Mössbauer spectroscopy and by extended X ray absorption fine structure gave evidence that large distributions of Fe sites and Fe–Fe distances exist for all the deuterides even those which were refined in the C15

[1]To whom correspondence should be addressed.
[2]Present address: Laboratoire de Cristallographie, 24 Quai E. Ansemet, 1211 Genève 4, Switzerland.

0022-4596/99 $30.00

structure (6). The origin of these structural distortions was discussed in relation with magnetostrictive properties of RFe_2 compounds (6).

The present neutron diffraction study completes these previous works on the YFe_2–D_2 system. The neutron diffraction technique is appropriate to determine the localization of the deuterium atoms and the magnetic properties of the deuterides. In addition, *in situ* ND experiments can be used to follow structural transitions as a function of temperature.

In the first part, we will report on the influence of a thermal treatment on the synthesis of $YFe_2D_{1.3}$ and $YFe_2D_{1.9}$ compounds, deuterated at room temperature, by *in situ* neutron diffraction experiments as a function of the temperature. These experiments have been performed with bulk samples in closed sample holders connected to a volumetric device to measure the pressure and the evolution of deuterium content versus temperature.

In the second part we will present the structural analysis of single phase YFe_2D_x deuterides ($x = 1.3$, 1.75, 1.9, and 2.6) by high resolution powder neutron diffraction at 300 K. For $x = 1.3$ and 1.9, which both display tetragonal distortions compared to the cubic C15 structure, the order–disorder transition which occurs at high temperature is studied by *in situ* neutron diffraction as a function of temperature.

2. EXPERIMENTAL

The conditions of preparation and characterization of the YFe_2 intermetallic compound are given in Ref. 4. About 8 g of YFe_2 was crushed and sieved to less than 63 μm under argon atmosphere and then introduced in a sample holder and outgased under vacuum (10^{-2} bar) for 16 h at 353 K. An activation pretreatment at higher temperature (48 h at 593 K) and better vacuum (1.3×10^{-9} bar) was also performed. However, whatever the pretreatment was, the XRD patterns of the deuterides, prepared by deuterium absorption at room temperature, always show a mixture of YFe_2 and a YFe_2D_y deuteride with larger D content than the total amount of absorbed deuterium. Single phase deuterides can be obtained by applying a thermal treatment at temperatures larger or equal to 408 K after the deuterium absorption at room temperature.

In order to understand the influence of the thermal treatment, two samples with $x = 1.3$ and 1.9 have been prepared by deuterium absorption at room temperature (nonannealed or NA samples) and heated in the neutron beam.

Then to determine the structure of the single phase deuterides by high resolution neutron diffraction experiments the samples have been prepared by deuterium absorption at higher temperature (473 K for $x = 1.3$ and 408 K for $x = 1.75$, 1.9, and 2.6) and single phase compounds were obtained as checked by XRD.

TABLE 1
Conditions of Sample Preparations and Temperature Variations *T* (K) versus Time (*t*) for the *In Situ* Neutron Diffraction Experiments

Compound	Deuterium absorption temperature	*T* (K)	*t* (mn)
$YFe_2D_{1.3}$	Room temperature	293 to 473	600
		473	180
		473 to 360	360
$YFe_2D_{1.9}$	Room temperature	303 to 453	540
		453 to 423	100
		423 to 453	100
		453 to 330	255

The *in situ* powder neutron diffraction experiments on the NA YFe_2D_x ($x = 1.3$ and 1.9) samples were performed on the position sensitive detector (PSD) diffractometer D1B at the Institut Laue Langevin (ILL). This diffractometer is equipped with 400 cells and spans 80° in 2θ, the wavelength was 2.523 Å. The diffraction patterns were registered every 5 min from 28 to 108° in 2θ with a step of 0.05° while heating or cooling the samples. During the neutron experiments the silica sample holders were placed in a furnace operating under vacuum ($P = 1.3 \times 10^{-7}$ bar) equipped with vanadium heating elements and shields. They were connected to a volumetric device in order to follow the pressure variation and therefore the evolution of the D content. The temperature cycles chosen for each sample are given in Table 1.

The neutron diffraction patterns of the single phase deuterides were registered at 300 K on the 3T2 diffractometer of the Laboratoire Léon Brillouin (LLB). The wavelength was 1.227 Å and the angular range was $6° < 2\theta < 125°$ with a step of 0.02°. The deuteride samples were contained in vanadium sample holders.

All the neutron diffraction patterns were refined using the profile matching or Rietveld refinement method with the program Fullprof (8). The profiles of the diffraction lines were fitted with a Pseudo-Voigt function.

3. EXPERIMENTAL RESULTS AND DISCUSSION

3.1. Influence of the Thermal Treatment on the Deuterides Synthesis

3.1.1. $YFe_2D_{1.3}$. At room temperature the neutron diffraction pattern of NA $YFe_2D_{1.3}$ is a mixture of two cubic C15 phases: 62% of YFe_2 ($a = 7.36$ Å) and 38% of YFe_2D_y ($a = 7.79$ Å). The cell parameter of the YFe_2D_y phase corresponds to that of $YFe_2D_{2.6}$. The evolution of the neutron diffraction patterns as a function of time and temperature is presented as a 3D plot on Fig. 1. Up to 400 K the positions and the intensities of the lines remain almost unchanged.

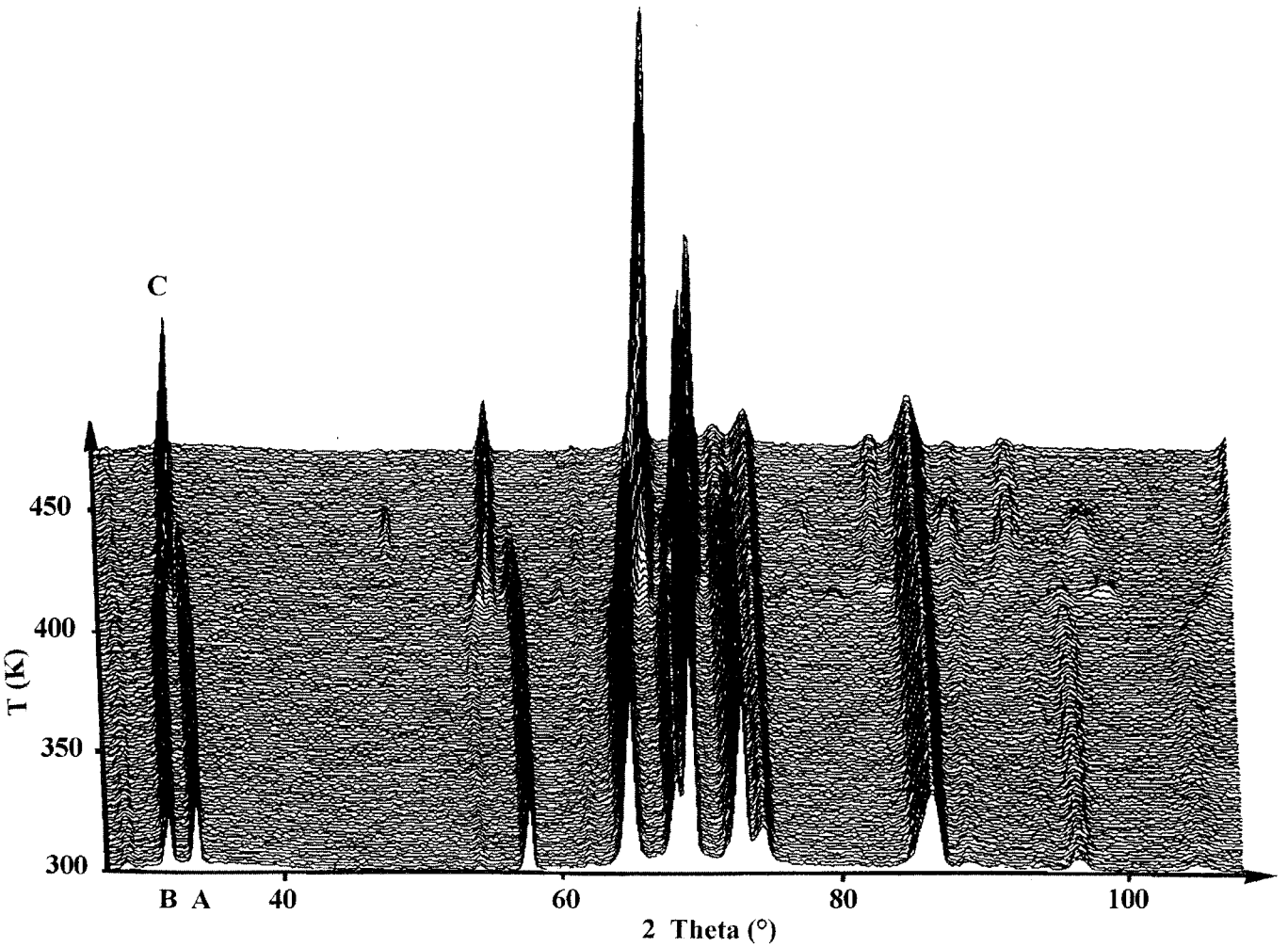

FIG. 1. 3D plot showing the evolution of the neutron diffraction patterns of NA $YFe_2D_{1.3}$ compound as a function of temperature during the heating process. A, B, and C correspond to lines belonging to YFe_2, $YFe_2D_{2.6}$, and $YFe_2D_{1.3}$, respectively.

Above 400 K the intensities of the YFe_2 lines start to decrease and their positions are shifted to lower angles. On the contrary the intensities of the $YFe_2D_{2.6}$ lines increase and their positions are shifted to larger angles. The growing of a new phase which is located between the two others is observed at the same time. A close examination of this plot indicates also the appearance and disappearance of some additional reflections between 414 and 460 K. At 473 K only one phase is observed.

In order to obtain quantitative results the ND patterns were refined with the Rietveld method. Each phase was assumed to crystallize in the cubic C15 structure and for the deuterides the position of the deuterium atom ($x = 0.339$, $y = 0.141$) was that refined for $YFe_2D_{2.6}$ (Table 5).

The evolution of the amount of each phase and of the cell parameters is plotted as a function of the temperature on Figs. 2a and 2b. The pressure variation measured during the experiment is added on Fig. 2a.

The amount of YFe_2 and $YFe_2D_{2.6}$ remains constant up to 400 K. Above this temperature the amount of YFe_2 decreases, the amount of $YFe_2D_{2.6}$ increases, and a second deuteride phase grows. The two deuteride phases merge into one phase at 425 K and above 460 K there is only one single deuteride phase.

The cell parameters of YFe_2 and $YFe_2D_{2.6}$ increase slightly and linearly up to 400 K. This variation can be attributed to the thermal expansion. Above 400 K, a larger increase of the YFe_2 cell parameter is observed up to 450 K, whereas the cell parameter of the YFe_2D_y phase decreases. The cell parameter of the second deuteride phase increases up to 425 K and then the two deuteride phases merge to form a single phase deuteride with $a = 7.64$ Å at 425 K. At 473 K there is only one phase with $a = 7.61$ Å.

The pressure (Fig. 2a) starts to increase above 370 K to reach a maxima at 404 K and then decreases again. Therefore the first changes in the neutron diffraction patterns

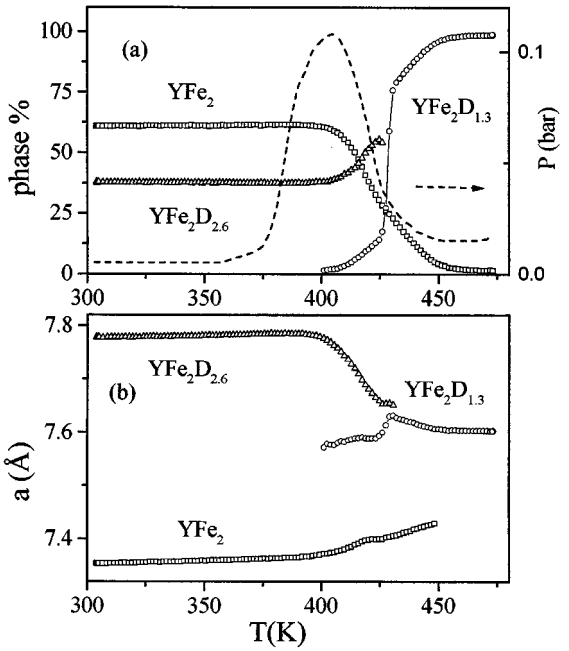

FIG. 2. Evolution of the amount of phases and of the pressure in the sample holder (a) and of the cell parameters (b) as a function of the temperature during the heating process for the NA $YFe_2D_{1.3}$ compound.

correspond to the maximum of the pressure. The calculated amount of deuterium desorbed by the sample in the gas phase is very small (5×10^{-3} D/f.u. at 404 K).

As mentioned before the appearance and disappearance of additional reflections were observed in the patterns (Fig. 1). As the cell parameter of the deuteride phase YFe_2D_y decreases from 7.79 to 7.64 Å, the deuterium content decreases and intermediate phases are formed. Some of the observed superstructure lines can be attributed to single phase $YFe_2D_{1.9}$ and then to $YFe_2D_{1.75}$ which are formed successively as the temperature increases as reported in Table 2. In addition superstructure lines belonging to the single phase $YFe_2D_{1.3}$ are observed from 400 to 460 K. Above 460 K, all the superstructure lines have disappeared and the patterns can be strictly indexed in the C15 structure.

TABLE 2

Temperature Ranges and Corresponding Cell Parameters of the Single Phase Deuterides at Which the Superstructure Lines Appears and Disappears during the Heat Treatment of the NA $YFe_2D_{1.3}$

Single phase compound	Temperature range (K)	Cell parameters (Å)
$YFe_2D_{1.3}$	410–430–460	7.59–7.64–7.61
$YFe_2D_{1.75}$	422–426	7.68–7.65
$YFe_2D_{1.9}$	414–420	7.73–7.69

3.1.2. $YFe_2D_{1.9}$. At room temperature the neutron diffraction pattern of $YFe_2D_{1.9}$ is a mixture of two C15 phases: 25% of YFe_2 ($a = 7.36$ Å) and 75% of YFe_2D_y ($a = 7.74$ Å). The cell parameter of the deuteride phase corresponds to a concentration of about 2.3 D/f.u.

Up to 425 K the positions and the intensities of the diffraction lines remain unchanged. Between 425 and 453 K the ND pattern evolution is similar to that observed for $x = 1.3$ and at 453 K only one phase is observed. The amount of phases and the cell parameter variations are plotted as a function of the temperature on Figs. 3a and 3b. The pressure variation measured during the experiment is added on Fig. 3a.

The amount of YFe_2 and $YFe_2D_{2.3}$ remains constant up to 425 K (Fig. 3a). Above this temperature the amount of YFe_2 decreases whereas the amount of the deuteride phase increases. A second deuteride phase $YFe_2D_{1.3}$ grows up to 440 K (4%) and decreases above. At 453 K there is only one single deuteride phase.

The cell parameters of YFe_2 and $YFe_2D_{2.3}$ increase slightly and linearly up to 425 K. Above 425 K, a larger increase of the YFe_2 cell parameter is observed up to 440 K, whereas the cell parameter of the YFe_2D_y phase decreases down to 7.70 Å. A new phase with $a = 7.55$ Å ($YFe_2D_{1.3}$) is formed above 425 K and its cell parameter increases slightly with the temperature.

The pressure variation (Fig. 3a) was found to increase slowly up to 380 K and faster from 380 to 410 K. Two small

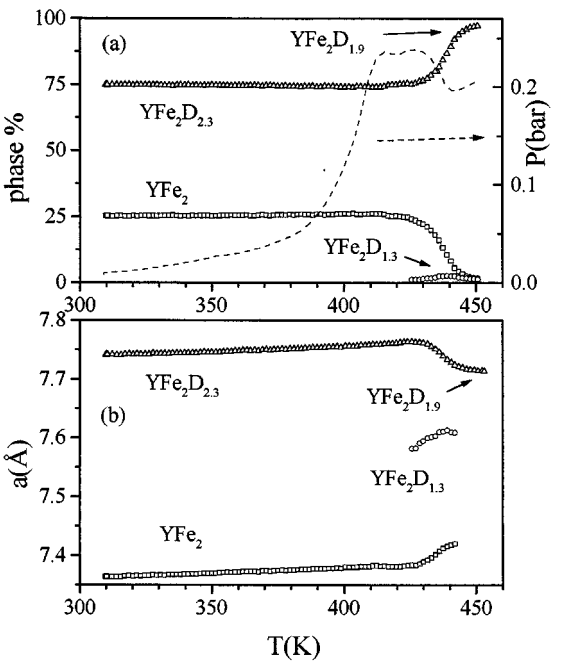

FIG. 3. Evolution of the amount of phases and of the pressure in the sample holder (a) and of the cell parameters (b) as a function of the temperature during the heating process for the NA $YFe_2D_{1.9}$ compound.

maxima are observed at 410 and 425 K and then the pressure decreases down to 440 K and increases again. The maximum pressure increase of 0.23 bar corresponds to 0.01 D/f.u. of desorbed deuterium, which is very small like for $YFe_2D_{1.3}$.

3.1.3. Discussion. For both compounds we observe above 400 K for $YFe_2D_{1.3}$ and 425 K for $YFe_2D_{1.9}$:

(i) a decrease of the amount of YFe_2 accompanied by an expansion of its cell parameter. This cell parameter increase can be explained by the formation of an α phase (solid solution of D in YFe_2) corresponding to a progressive increase of the deuterium solubility as a function of the temperature.

(ii) the formation of a second deuteride phase with $a = 7.55$ Å, which corresponds to a deuterium content below 1.3 D/f.u. In the case of the NA $YFe_2D_{1.3}$ sample this additional phase grows until a single phase deuteride is formed, whereas for the other sample ($x = 1.9$) this phase disappears above 450 K. According to the YFe_2–H_2 phase diagram, this phase corresponds to the first deuteride that can be formed starting from YFe_2.

In addition, for the two nonannealed samples the amount of deuteride phase (38% of $YFe_2D_{2.6}$ for $x = 1.3$ D/f.u and 75% of $YFe_2D_{2.3}$ for $x = 1.9$ D/f.u.) is lower than it should be expected from the total D content (50 and 83%, respectively). This discrepancy can be explained by the presence of a poorly crystalline $YFe_2D_{1.3}$ phase, which gives only an amorphous contribution to the background and cannot be separated from the contribution of the amorphous silica container. As the sample is heated this amorphous phase can crystallize leading to the growing of the intermediate $YFe_2D_{1.3}$ phase.

(iii) the decrease of the cell parameter of the YFe_2D_y phase, indicating a decrease of its deuterium content, is accompanied by an increase of the amount of this phase. Such evolution can be explained by a mechanism of deuterium diffusion inside a grain.

As for both $YFe_2D_{1.3}$ and $YFe_2D_{1.9}$ compounds the pressure increase corresponds to a very small deuterium desorption (< 0.02 D/f.u.); this indicates that the deuterium desorption in the gas phase followed by a deuterium reabsorption is negligible. The mechanism of the deuteride formation is therefore an intragrain diffusion process. This means that at room temperature each grain is formed by a core of YFe_2 or α phase surrounded by a deuterium-rich phase. The heating process makes it possible to initiate the advance of the boundary between the two phases toward the center of the grain. This occurs at the expense of the deuterium-rich phase for which the deuterium content decreases.

3.2. Study of Single Phase YFe_2D_x Deuterides ($x = 1.3$, 1.75, 1.9, and 2.6)

3.2.1. $YFe_2D_{1.3}$. The $YFe_2D_{1.3}$ XRD pattern was refined in a tetragonal structure ($a = 11.985(2)$ Å and $c = 7.622\ (1)$ Å) within the $I\bar{4}$ space group with four different sites for the Y atoms and 5 for the Fe atoms (3). The neutron diffraction (ND) pattern of this compound (Fig. 4a) clearly shows superstructure lines, with larger intensities than in the XRD pattern. All these lines can be indexed in the tetragonal structure. To fully refine this ND pattern we have to take into account, in addition to the Y and Fe atomic positions, both the deuterium contribution and the ferromagnetic moment of the Fe atoms. Assuming that the deuterium atoms are filling A2B2 interstitial sites, the 96-g position in the $Fd\bar{3}m$ space group splits into 30 different 8-g positions in the $I\bar{4}$ space group. Considering a statistical occupation of all the deuterium atoms in these 30 sites leads to a poor agreement with the experimental data ($R_B = 29\%$). The occupation factors of the deuterium atoms were therefore refined and only seven deuterium sites were found to be significantly occupied. Their positions were also refined, showing some displacement relative to the positions derived of the C15 structure. The magnetic structure was refined assuming a ferromagnetic alignment of all the Fe moments. Although Mössbauer data (5) indicate different hyperfine fields for each Fe sites, it was not possible to refine independently the moment of the five Fe sites. A mean magnetic moment of 1.45 μB/Fe was obtained close to the magnetic moment measured at room temperature. Results of the refinement are reported in Table 3 and the refined pattern is displayed on Fig. 4a.

Analyzing separately the contribution of the nuclear and magnetic intensities to the ND pattern indicates that the superstructure lines are due to the nuclear contribution of the metal and deuterium atoms, whereas the magnetic intensity is contained in the lines which could be indexed in the C15 structure.

The evolution of the structure of $YFe_2D_{1.3}$ has been followed by ND as a function of the temperature and the evolution of the ND patterns is presented in Fig. 5.

From 473 down to 460 K the ND patterns of $YFe_2D_{1.3}$ can be refined in the cubic C15 structure with D atoms located in the A2B2 site (96 g). In addition it is necessary to introduce a ferromagnetic contribution for the Fe atoms with a moment of 1.6(2) μB to refine correctly these patterns. Below 460 K, superstructure lines belonging to the tetragonal cell of $YFe_2D_{1.3}$ appears as the temperature decreases. The ND patterns were therefore refined below 460 K in this tetragonal structure and the cell parameters evolution as a function of the temperature is displayed on Fig. 6. For sake of clarity, $a_T \times \sqrt{2/5}$, which can be directly compared to a_c, has been reported in Fig. 6. The tetragonal distortion increases as the temperature decreases from 460 to 445 K. Below 445 K the linear decrease of the cell parameters with temperature can be explained by the thermal contraction. This thermal variation shows some anisotropy since it is three times larger along the a axis ($\Delta a_T/\Delta T = 2.6 \times 10^{-4}$) than along the c axis ($\Delta c_T/\Delta T = 8.6 \times 10^{-5}$). At the

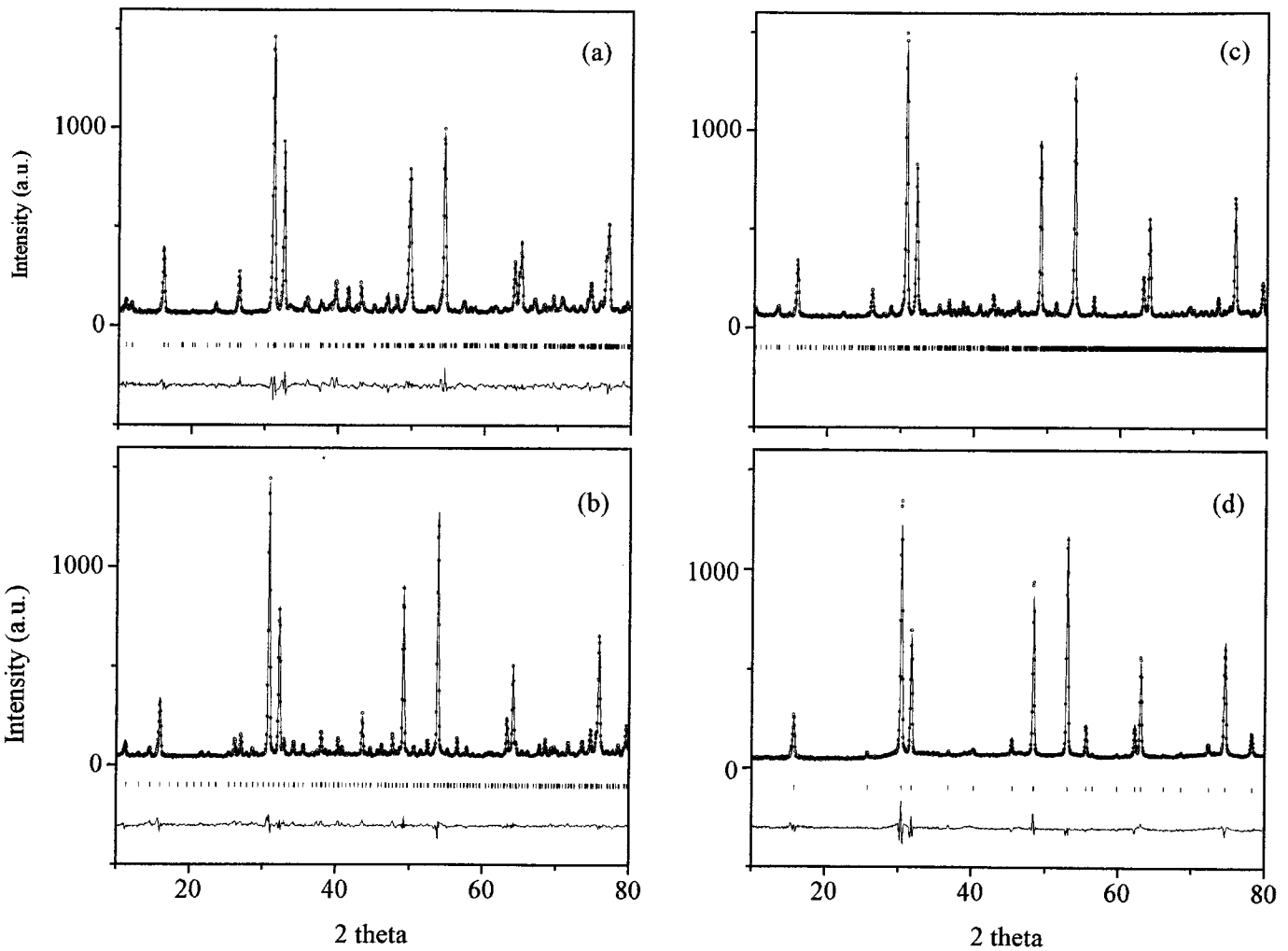

FIG. 4. Neutron diffraction patterns of (a) $YFe_2D_{1.3}$, (b) $YFe_2D_{1.75}$, (c) $YFe_2D_{1.9}$, and (d) $YFe_2D_{2.6}$: (o) experimental patterns and (|) ticks indicating the positions of the reflection lines. For $YFe_2D_{1.75}$, $YFe_2D_{1.3}$, and $YFe_2D_{2.6}$ the calculated patterns (—) were obtained by Rietveld refinement and the difference curves are presented below. For $YFe_2D_{1.9}$, the calculated pattern was obtained by profile matching.

structural transition we observe a small volume anomaly but without significant thermal hysteresis effect, since the superstructure lines corresponding to this phase disappear at the same temperature (460 K) during the heating process.

3.2.2. $YFe_2D_{1.75}$. Both XRD and ND patterns of $YFe_2D_{1.75}$ can be refined in the $I\bar{4}3m$ space group ($Z = 64$) within a double cubic cell ($a = 15.336(2)$ Å). The Y and Fe atomic positions were first refined in the XRD pattern and used to refine the ND pattern. We have assumed that the deuterium atoms were located in A2B2 sites, which corresponds to one 96-g site in the $Fd3m$ space group. This 96-g site corresponds to 20 different sites in the cubic cell (8 sites 24 g and 12 sites 48 h). A statistical occupation of the deuterium atoms in all the A2B2 sites leads to a poor structural agreement ($R_B = 25\%$). A good refinement of the pattern was obtained with only 9 partially occupied sites among the available 20 sites, which indicates an ordering of the D atoms in some preferential A2B2 sites. A ferromagnetic structure was also introduced for the Fe atoms and a mean Fe moment of 1.9(1) μB/Fe was obtained. This value is larger than the mean value obtained from bulk magnetic measurements (1.5 μB/Fe). However like for $YFe_2D_{1.3}$, although Mössbauer experiments have indicated different hyperfine fields, it was not possible to refine independently the magnetic moment for each Fe site. Results of the refinement are reported in Table 4 and the refined pattern is shown on Fig. 4b.

We also observe for this compound that the intensity of the superstructure lines is due to the nuclear contribution of the atoms, i.e., the positions of the Y and Fe atoms which are shifted from the positions calculated in the C15 structure

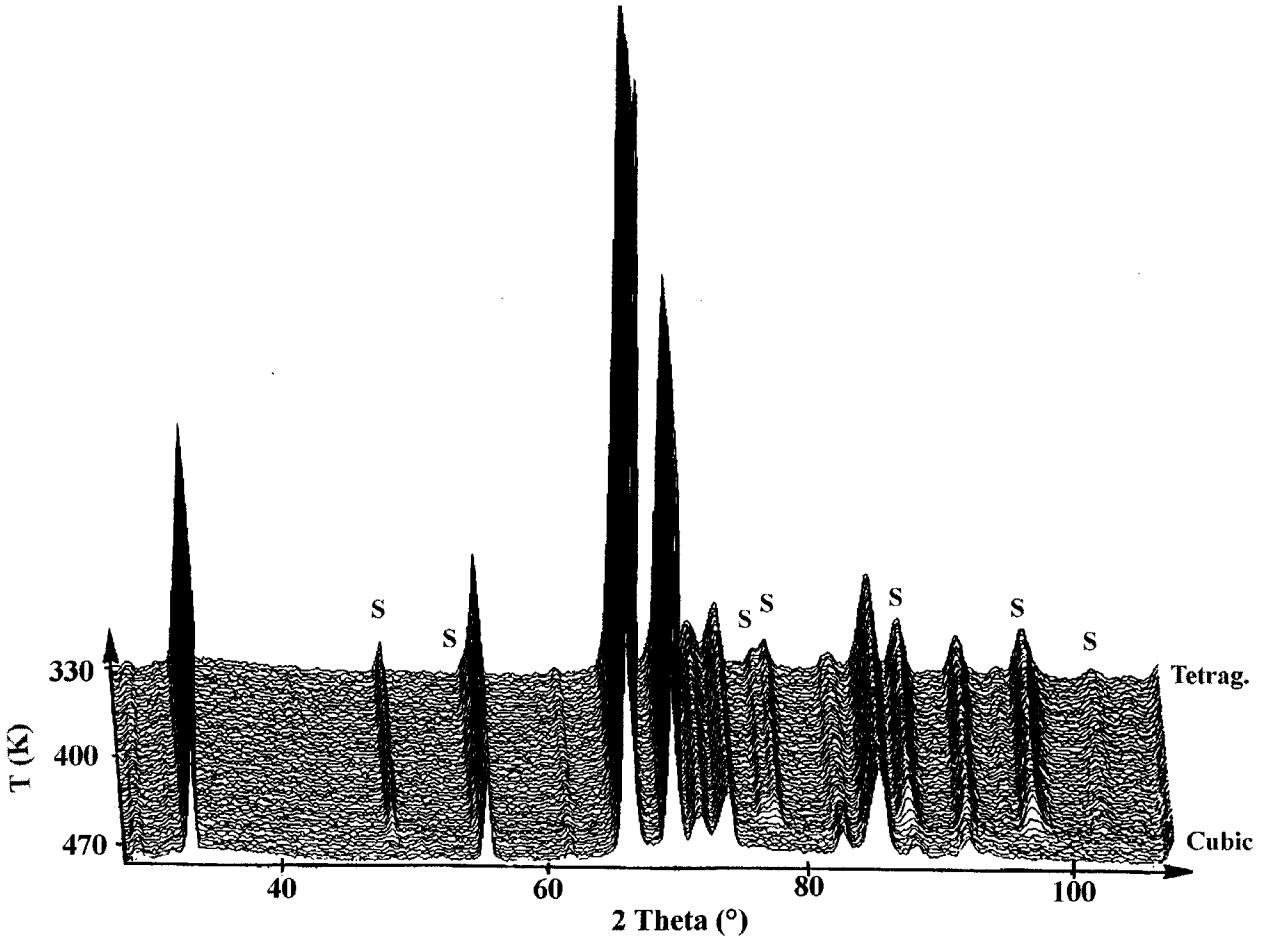

FIG. 5. Evolution of the neutron diffraction patterns of the $YFe_2D_{1.3}$ compound showing the apparition of the superstructure lines (S) belonging to the tetragonal structure as the temperature decreases.

and the ordering of deuterium atoms, whereas the magnetic intensity contributes mainly to lines that could be indexed in the C15 structure.

3.2.3. $YFe_2D_{1.9}$. The ND pattern of $YFe_2D_{1.9}$ (Fig. 4c) clearly shows several superstructure lines in addition to the lines belonging to the C15 structure. However, since it was not possible to index all these superstructure lines by doubling the cubic cell parameter as proposed earlier (4) a new cell was searched. Finally, it was possible to index all the lines of both XRD and ND patterns in a body centred tetragonal cell with $a_T = a_C \times \sqrt{5/2} = 12.145(2)$ Å and $c_T = 3a_C = 23.064(2)$ Å, where a_T and c_T are the tetragonal parameters and a_c is the C15 cubic cell parameter ($a = 7.684$ Å). This new tetragonal cell is three time larger than the tetragonal cell of $YFe_2D_{1.3}$ along the c axis, but exhibits a weaker tetragonal distortion ($c_T/a_T \times \sqrt{5/18} = 1.00074$ for $x = 1.9$) compared to ($c_T/a_T \times \sqrt{5/2} = 1.00438$ for $x = 1.3$). This cell can also be described in the $I\bar{4}$ space group, leading to 12 different sites for the Y atoms and 15 different sites for the Fe atoms. Due to the weakness of the superstructure lines in the XRD pattern and to the large amount of the atomic positions it was not possible to refine the Y and Fe atomic positions. However, like for $YFe_2D_{1.3}$ and $YFe_2D_{1.75}$ the superstructure lines should arise from the displacement of Y and Fe atoms and from deuterium ordering.

The evolution of the structure $YFe_2D_{1.9}$ as a function of temperature was also studied by *in situ* neutron diffraction. From 453 down to 426 K the ND pattern can be refined in the C15 structure with deuterium atoms located in the A2B2 site (96 g). As for $YFe_2D_{1.3}$ above its structural transition, a correct refinement can be obtained only with a ferromagnetic contribution of 1.7(2) μB for the Fe atoms. Below 426 K we observe the apparition of superstructure lines which are indexed in the tetragonal cell of $YFe_2D_{1.9}$. The evolution of the intensity of the (415) superstructure line ($d = 2.49$ Å at 330 K) as a function of time and temperature (Fig. 7a) shows a thermal hysteresis of 16 K ($Ts = 444$ K on heating and 427 K on cooling), which indicates the first order character of the transition. Since for this compound

TABLE 3
Results of the Refinement of the $YFe_2D_{1.3}$ ND Pattern

Atom		x	y	z	B	N_{occ}
Y1	(2a)	0	0	0	0.67(5)	2
Y2	(2b)	0	0	1/2		2
Y3	(8g1)	0.596	0.712	0.736		8
Y4	(8g2)	0.907	0.286	0.517		8
Fe1	(8g3)	0.957	0.906	0.612	0.46(3)	8
Fe2	(8g4)	0.952	0.408	0.138		8
Fe3	(8g5)	0.853	0.706	0.612		8
Fe4	(8g6)	0.859	0.210	0.127		8
Fe5	(8g7)	0.767	0.021	0.153		8
D1	(8g8)	0.695(2)	0.737(2)	0.486(3)	1.36(2)	5.2(3)
D2	(8g9)	0.797(2)	0.606(2)	0.135(1)		5.7(3)
D3	(8g10)	0.775(4)	0.896(3)	0.206(5)		2.9(3)
D4	(8g11)	0.747(3)	0.774(3)	0.726(4)		4.0(3)
D5	(8g12)	0.868(2)	0.955(3)	− 0.017(5)		4.1(3)
D6	(8g13)	0.949(2)	0.656(2)	0.008(3)		6.5(4)
D7	(8g14)	0.357(2)	0.415(2)	0.284(3)		6.5(3)
D/f.u.		1.7(0.2)				
M/Fe (μ_B)		1.45(9)				
a (Å)		11.985(2)	c (Å)	7.622(1)		SG: $I\bar{4}$
R_{profil}		6.49%	R_{Bragg}	9.04%	$R_{magnetic}$	7.30%

Note. a and c are the cell parameters, x, y, and z the atomic coordinates, B the Debye Waller factors, N the occupation factors in the cell, R_{profil}, R_{Bragg}, and $R_{magnetic}$ the profile, Bragg, and magnetic factors of agreement, respectively.

TABLE 4
Results of the Refinement of the $YFe_2D_{1.75}$ ND Pattern

Atom		x	y	z	B	N_{occ}
Y1	(2a)	0	0	0	0.24(5)	2
Y2	(6b)	0	1/2	1/2		6
Y3	(8c1)	0.127	0.127	0.127	0.71(3)	8
Y4	(24g1)	0.260	0.260	0.006		24
Y5	(24g2)	0.135	0.135	0.384		24
Fe1	(8c2)	0.315	0.315	0.315		8
Fe2	(24g3)	0.302	0.302	0.816		24
Fe3	(24g4)	0.074	0.074	0.818		24
Fe4	(24g5)	0.070	0.070	0.319		24
Fe5	(48h1)	0.056	0.310	0.560		48
D1	(24g6)	0.241(2)	0.241(2)	0.119(2)	0.62(8)	4(0.6)
D2	(24g7)	0.512(2)	0.512(2)	0.133(1)		10.9(0.5)
D3	(24g8)	0.107(3)	0.107(3)	0.496(3)		5.2(0.6)
D4	(24g9)	0.018(1)	0.018(1)	0.142(1)		16.4(0.5)
D5	(48h2)	0.502(1)	0.389(1)	0.241(1)		36.7(1.0)
D6	(48h3)	0.092(3)	0.272(3)	0.158(4)		8(0.8)
D7	(48h4)	0.354(2)	0.008(2)	0.141(1)		17.2(0.8)
D8	(48h5)	0.133(2)	0.029(2)	0.239(2)		15.7(0.9)
D9	(48h6)	0.129(1)	0.378(1)	0.242(2)		14.8(0.8)
D/f.u.		2.0(0.1)				
M/Fe (μB)		1.90(6)				
a (Å)		15.336 (2)	SG: $I\bar{4}3m$			
R_{profil}		5.35%	R_{Bragg}	8.7%	$R_{magnetic}$	6.9%

Note. a is the cell parameters, x, y, and z the atomic coordinates, B the Debye Waller factors, N the occupation factors in the cell, R_{profil}, R_{Bragg}, and $R_{magnetic}$ the profile, Bragg, and magnetic factors of agreement, respectively.

the tetragonal distortion is very weak, the ND patterns were refined in the mean cubic structure. The variation of the cell parameter (Fig. 7b) indicates also a small magnetovolume effect at the transition.

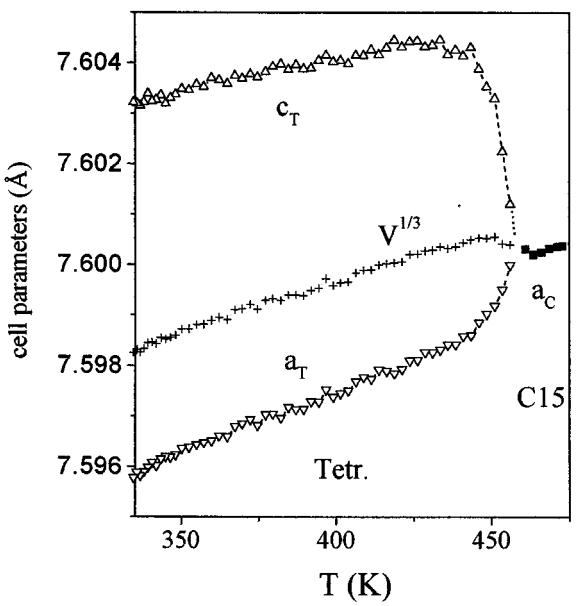

FIG. 6. Evolution of the cell parameters of the cubic and tetragonal phases of $YFe_2D_{1.3}$ as a function of temperature.

3.2.4. $YFe_2D_{2.6}$. For $YFe_2D_{2.6}$ both the XRD and the ND patterns can be refined in the cubic C15 type structure with $a = 7.785$ (2) ($Fd\bar{3}m$ SG) without any superstructure lines. The results of the refinement are reported in Table 5 and the refined pattern is displayed in Fig. 4d. The deuterium atoms are located in the tetrahedral A2B2 sites (96-g position) and the deuterium content (2.5(1) D/f.u.) is in agreement with the deuterium concentration measured by the volumetric method. In addition the refined Fe magnetic moment of 1.8 μB/Fe is close to the 1.6 μB/Fe obtained from bulk magnetic measurements.

3.2.5. Discussion. The three single phase deuterides, $YFe_2D_{1.3}$, $YFe_2D_{1.75}$, and $YFe_2D_{1.9}$, display at room temperature superstructure lines which can be indexed in different structures derived from the C15 structure. $YFe_2D_{1.3}$ crystallizes in a centered tetragonal structure with $a =$ 11.98 Å and $c = 7.62$ Å (SG $I\bar{4}$), $YFe_2D_{1.75}$ in a centered cubic structure (SG $I\bar{4}3m$) with $a = 15.33$ Å and $YFe_2D_{1.9}$ in a tetragonal structure with $a = 12.15$ Å and $c = 23.06$ Å (SG $I\bar{4}$). It is worth to notice that as the deuterium content increases, the size of the superstructure cell increases along the "c axis" in the sequence a_c, $2a_c$, and $3a_c$, where a_c, represents the lattice parameter of the C15 structure.

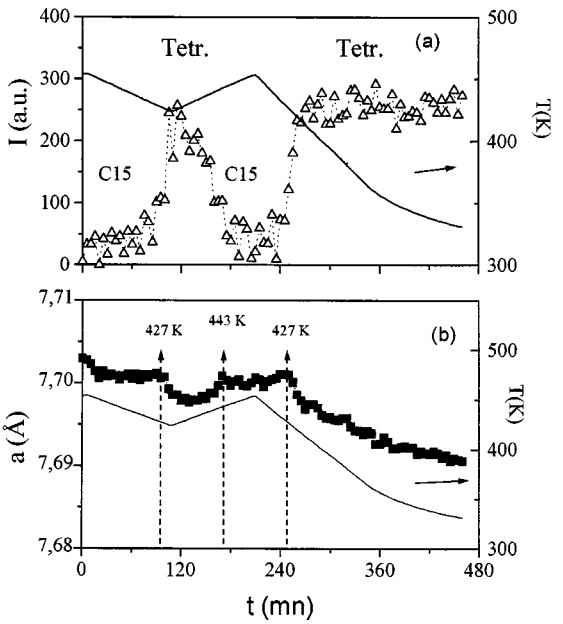

FIG. 7. Evolution versus time of the intensity of the (415) superstructure line (a) and of the cubic cell parameter (b) of $YFe_2D_{1.9}$ during the temperature cycles. The temperature variation is added with the scale on the right axis.

The analysis of the ND patterns of $YFe_2D_{1.3}$ and $YFe_2D_{1.75}$ at 300 K has shown that the deuterium atoms are preferentially located in some interstitial A2B2 sites, indicating an ordering of the D atoms. This deuterium ordering is more pronounced for $x = 1.3$ than for $x = 1.75$ since a smaller amount of sites are occupied with a larger occupation rate. In addition for both compounds we have observed that the intensity of the superstructure lines originates from the displacement of the Y and Fe atoms and the deuterium contribution. Although the structure of $YFe_2D_{1.9}$ could not be solved due to the weakness of the superstructure lines, deuterium ordering is also expected for this compound. The change of symmetry between tetragonal ($x = 1.3$ and 1.9) and cubic ($x = 1.75$) structures should therefore be related to different possibilities of ordering deuterium atoms inside the lattice. If a more symmetric structure is obtained for $x = 1.75$, it means that for this concentration the partial ordering of D atoms is also more symmetric and thermodynamic calculations could be useful in explaining this result.

TABLE 5
Results of the Refinement of the $YFe_2D_{2.6}$ ND Pattern

Atom		x	y	z	B	N
Y	(8a)	1/8	1/8	1/8	1.47(3)	1
Fe	(16d)	1/2	1/2	1/2	1.55(2)	2
D	(96g)	0.339(2)	0.339(2)	0.141(4)	1.43(10)	2.5(1)
M/Fe	(μB)	1.77(3)				
a (Å)		7.785(2)	SG $Fd\bar{3}m$			
R_{profil}		5.17%	R_{Bragg}	8.45%	$R_{magnetic}$	8.76%

Note. a is the cell parameters, x, y, and z the atomic coordinates, B the Debye Waller factors, N the occupation factors in the cell, R_{profil}, R_{Bragg}, and $R_{magnetic}$ the profile, Bragg, and magnetic factors of agreement, respectively.

The *in situ* ND experiments for $YFe_2D_{1.3}$ and $YFe_2D_{1.9}$ have shown the disappearance of the superstructure lines above 460 and 444 K, respectively. Above these temperatures their ND patterns can be refined in a C15 structure with a statistical occupation of the D atoms in A2B2 sites and a ferromagnetic contribution of the Fe atoms. This indicates that for both compounds this order–disorder transition is related to the ordering of deuterium atoms rather than to magnetic ordering.

In previous studies (5, 6), we have proposed that these structural transitions were caused by magnetic ordering since in the case of $YFe_2D_{3.5}$ the rhombohedral distortion occurs just below the Curie temperature (3, 9). This was also supported by the magnetostrictive properties of several RFe_2 intermetallic compounds (R = Sm, Tb, Er, and Tm), for which tetragonal or rhombohedral distortions are observed below their Curie temperature (10). This ND study shows that in fact for YFe_2D_x deuterides with low D content ($1.3 \leq x \leq 1.9$) the structural transitions are rather related to the order of the deuterium atoms. This deuterium ordering induces a displacement of the Y and Fe atoms to accommodate the size of the occupied deuterium sites. In addition since above the structural transition temperatures a cubic C15 structure is observed, it is possible that the transition temperatures correspond to a critical temperature in the PCT isotherm, i.e., that a solid solution behavior is observed for higher temperatures. This is supported by the fact that the YFe_2 isotherm at 473 K does not display any more plateau above 1 D/f.u., whereas plateaus are observed for the isotherms at lower temperature (353 and 408 K) (4).

Local order studies by EXAFS (6) have shown that for all these deuterides a large distribution of Fe–Fe distances has to be taken into account. In addition Mössbauer spectroscopy experiments for $x = 1.3$, 1.75, and 1.9 have shown the existence of different Fe sites with different isomer shifts and hyperfine fields. This can be explained by the fact that each Fe site is surrounded by a different number of deuterium atoms and Fe neighbors at different distances ($2.4\ \text{Å} < d_{Fe\text{–}Fe} < 2.95\ \text{Å}$). The variation of the isomer shift can be related to a change of the s density at the ^{57}Fe nuclei and to volume variation induced by the deuterium atoms. The hyperfine field is related to the magnetic moment of the Fe atom, which is very sensitive to the Fe–Fe distances: larger Fe–Fe distances generally induce a larger magnetic moment. Therefore the distribution of hyperfine field reflects the distribution of Fe distances.

In the case of $YFe_2D_{2.6}$ both XRD and ND studies show that this compound crystallizes in the cubic C15 structure without any superstructure lines, whereas Mössbauer spectroscopy and EXAFS experiments indicate several Fe sites with different chemical environments like in the other deuterides. The reason for this discrepancy is probably that these local structural defects are not long-range ordered and that diffraction techniques show only an averaged structure. This is also supported by the broadening of the Mössbauer lines, which is an indication that the Fe site distribution becomes broader for larger D content.

The analysis of the ND pattern for $x = 1.3$, 1.75, and 2.6 gives only a mean ferromagnetic structure with a magnetic moment varying from 1.45 to 1.8 μB. Significant magnetic intensity is observed only for diffraction lines which could be indexed in the C15 structure. This indicates that the mean magnetic structure is closely related to that of YFe_2, i.e., to a ferromagnetic structure.

4. CONCLUSION

In situ ND experiments have been performed on "non-annealed" $YFe_2D_{1.3}$ and $YFe_2D_{1.9}$ samples in order to study the influence of the thermal treatment on the deuterides synthesis. After deuterium absorption at room temperature, the samples are a mixture of YFe_2 and a deuteride phase. An appropriate heat treatment makes it possible to obtain single phase deuterides by a mechanism of deuterium diffusion inside a grain.

Single phase $YFe_2D_{1.3}$, $YFe_2D_{1.75}$, and $YFe_2D_{1.9}$ deuterides crystallize at room temperature with superstructures which disappear above critical temperatures (460 K for $x = 1.3$ and 444 K for $x = 1.9$). The origin of these order–disorder transitions has to be related rather to deuterium ordering than to magnetic ordering, since the compounds are still ferromagnetic above these transitions. $YFe_2D_{2.6}$ crystallizes in the C15 structure with deuterium atoms statistically located in A2B2 interstitial sites. Since Mössbauer data have shown a distribution of Fe sites for all these deuterides, local structural distortions should also exist for $YFe_2D_{2.6}$, but they are averaged at long-range order (6). The change of symmetry between tetragonal ($x = 1.3$ and 1.9) and cubic ($x = 1.75$, 2.6) structures of the deuterides should be related to different possibilities of ordering deuterium atoms inside the lattice and thermodynamic calculations will be undertaken to explain the stability of each phase.

REFERENCES

1. A. Kierstead, *J. Less Common Met.* **71,** 303 (1980).
2. T. B. Flanagan, J. D. Clewley, N. B. Mason, and H. S. Chung, *J. Less Common Met.* **130,** 309, (1987).
3. D. Fruchart, Y. Berthier, T. de Saxe, and P. Vuillet, *J. Less Common Met.* **130,** 89, (1987).
4. V. Paul-Boncour, M. Latroche, L. Guénée, and A. Percheron-Guégan, *J. Alloys Comp.* **255,** 195 (1997).
5. V. Paul-Boncour, L. Guénée, M. Latroche, M. Escorne, A. Percheron-Guégan, Ch. Reichl, and G. Wiesinger, *J. Alloys Comp.* **253–254,** 272 (1997).
6. V. Paul-Boncour, L. Guénée, M. Latroche, M. Escorne, A. Percheron-Guégan, Ch. Reichl, and G. Wiesinger, *J. Alloys Comp.* **262–263,** 45 (1997).
7. H. M. Rietveld, *Acta Crystallogr.* **22,** 151 (1967).
8. J. Rodriguez-Carjaval, *in* "Union of crystallography" (Eds.), p. 127. Abstracts of Satellite Meeting on Powder Diffraction, Toulouse, France, 1990.
9. M. Latroche, V. Paul-Boncour, A. Percheron-Guégan, and F. Bourée-Vigneron, *J. Solid State Chem.* **133,** 568 (1997).
10. B. Barbara, J.P. Giraud, J. Laforest, R. Lemaire, E. Siaud, and J. Schweitzer, *Physica* **86/88 B,** 155 (1977).